Bearing capacity of tall monopile offshore wind turbine towers under environmental loading

Hu, Yu; Yang, Jian; Baniotopoulos, Charalampos

DOI:
10.1007/978-981-16-7735-9_46

Bearing Capacity of Tall Monopile Offshore Wind Turbine Towers under Environmental Loading

Y. Hu[a,b], J. Yang[a,b] and C. Baniotopoulos[b]

[a]School of Naval Architecture, Ocean and Civil Engineering, Shanghai Jiao Tong University, Shanghai 200240, China

[b]School of Civil Engineering, University of Birmingham, Edgbaston, Birmingham, B15 2TT, U.K.

Abstract

Offshore wind energy is a rapidly maturing renewable energy technology that is poised to play an important role in future energy systems. The respective advances refer among others to the monopile foundation that is frequently used to support wind turbines in the marine environment. In the present research paper, the structural response of tall wind energy converters with various stiffening schemes is studied during the erection phase as the latter are manufactured in modules that are assembled in situ. Rings, vertical stiffeners, T-shaped stiffeners and orthogonal stiffeners are considered efficient stiffening schemes to strengthen the tower structures. The loading bearing capacity of offshore monopile wind turbine towers with the four types of stiffeners were modeled numerically by means of finite elements. Applying a nonlinear buckling analysis, the ultimate bearing capacity of wind turbine towers with four standard stiffening schemes were compared in order to obtain the optimum stiffening option.

Keywords: offshore wind turbine tower; loading bearing capacity; stiffening scheme; offshore wind turbine tower erection

1. Introduction

Wind energy already significantly contributes to the reduction of greenhouse negative effects while contributing to economic growth in many countries as a leading solution against climate change globally. Offshore wind energy has been developing rapidly in the world, whilst Europe as the leader in offshore wind energy has the potential to realize up to 3400 TWh of offshore wind energy within its waters in 2030 [1]. In order to keep the monopile as thin as possible, the tower can be stiffened in different ways by various stiffening schemes to resist all possible loadings e.g., the wind, the current and the wave loadings in marine environments. For wind turbine towers, stiffening schemes can be employed to strengthen the tubular towers. Several researchers studied this research topic and proposed various methods to strengthen the tower structure in order to either decrease the cost of the tower or improve its structural response. Stavridou et al. [2] examined ring stiffeners and vertical stiffening schemes to eliminate the presence of short wavelength buckles of the tower due to bending. Gkantou et al. [3] performed the life cycle assessment of tall hybrid onshore steel wind turbine towers. Hu et al. [4-9] performed mechanical characteristics of onshore and offshore wind turbine towers under environmental loads stiffened by different stiffening solutions.

Tubular wind turbine towers are often employed as supporting structures to resist failure under external loadings; therefore, buckling analysis should be examined to explore their bearing capacity. Jay et al. [10] performed a program of flexural buckling tests of tapered circular steel wind towers with diameters between 0.7 and 1.1 m and maximum diameter-to-thickness ratios between 200 and 350 and concluded that location and orientation of the local buckling region were correlated with the spiral seam welds on the specimens. All the aforementioned studies focus on the bearing capacity and the buckling of the wind turbine system, however, they have not considered the buckling analysis and bearing capacities of the wind turbine towers during the critical erection phase. In the present study the bearing capacity of tubular wind turbine steel towers during the erection phase subjected to horizontal, vertical and bending loadings are investigated and the effect of various stiffening schemes in their ultimate bearing capacity in the marine environment is studied.

3. Bearing Capacity of the Offshore Tower with Stiffeners

3.1. Tower Models

For offshore wind turbine towers, the stiffeners are often employed to stiffen the tower wall. To compare the effect of the various stiffeners schemes on the structural performance of the offshore towers during the erection phase, towers with four stiffening schemes including a tower with rings, a tower with vertical stiffeners, a tower with T-shaped stiffeners and a tower with orthogonal stiffeners regarded, respectively, as tower I, tower II, tower III and tower IV were investigated. Figures 1 and 2 describe the geometry of the offshore wind turbine towers I, II, III and IV at hand. According to Figures 1 and 2, the height of the tower is 73.39 m, the top and bottom diameters of the towers are, respectively, 3276 mm and 5200 mm. For tower I, its ring spacing is 9 m and it contains eight rings along the tower wall. The width and thickness of these rings are 200 mm and 100 mm, respectively. For vertical stiffeners, its width and thickness are, respectively, 200 mm and 100 mm as shown in Figure 2 and the other edge of the vertical stiffeners is parallel to tower edge as shown in Figure 1. The four vertical stiffeners are distributed uniformly in the tower wall. The lengths of T shaped stiffeners in two sides are, respectively, 100 mm and 200 mm as displayed in Figure 2. The thickness of T shaped stiffeners is 50 mm. For tower IV, the ring spacing of orthogonal stiffeners is 11m and its four vertical stiffeners are also distributed uniformly in a similar way as in Tower II. The material property of FE model is Q345 steel as shown in Table 1.

For the FE models of the tower, the tie constraint was used to connect the stiffeners and the shell, i.e., the tower wall by using ABAQUS software [12]. The tower bottoms were considered to be fully fixed. On the top of the tower models, the circle center of the tower top can be setup to couple the top circle of the tower to the reference point. On the top, the tower is subjected to gravity and moment due to the eccentricity of wind turbines and the horizontal force resultant from wind loadings applied to blades of the wind turbine. The gravity, horizontal force and moment applied to the 73.39 m offshore tower are, respectively, 762,140 N, 1.0×10^6 N and 3.9479×10^8 N·mm. The tower should resist the gravity, the moment and the horizontal force on the top and therefore, its bearing capacity of the tower should be evaluated. In the present study, four stiffeners schemes are compared to explore the optimum stiffening option for the tower wall.

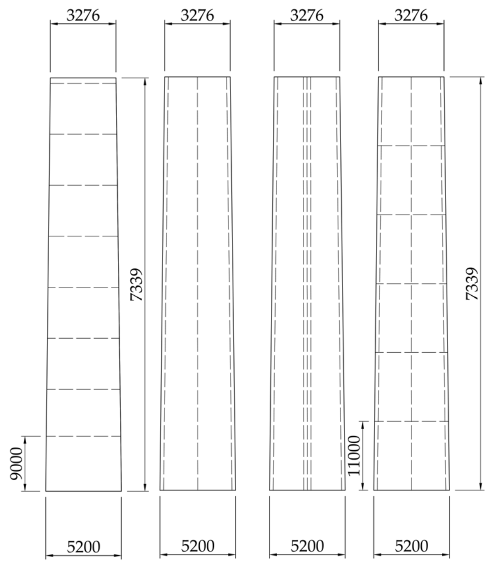

Figure 1. Geometric data of the towers with the four stiffening schemes (in mm).

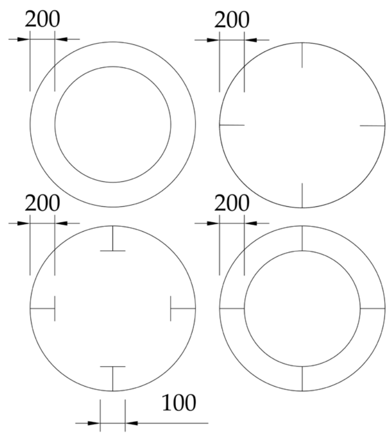

Figure 2. Geometric data of the stiffeners in the cross-section view of the tower (in mm).

Table 1. The material properties of steel.

Material	Density	Elasticity Module	Poisson's Ratio	Yield Stress	Plastic Strain
Steel	7.85 g/cm^3	205 GPa	0.3	345 GPa	0
				428 GPa	0.1

3.2. Stiffeners Mass

To compare the different stiffening options, the rings, vertical stiffeners, T-shaped stiffeners and orthogonal stiffeners should have all the same mass in order to study their efficacy. As the T-shaped stiffeners and the orthogonal stiffeners geometrically are based on the initially designed rings and vertical stiffeners, their mass can also be obtained by using the mass formula of rings and vertical stiffeners. In Figure 3 the geometry of the tower with rings and vertical stiffeners is presented.

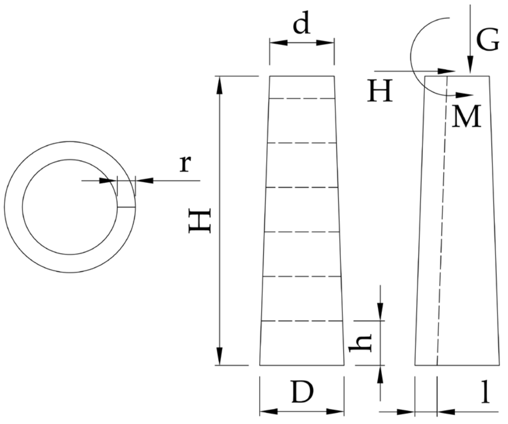

Figure 3. Geometry of the tower with rings and vertical stiffeners.

In the model at hand

$$M_r = \pi r T\{\left[nD - \frac{(D-d)h}{2H}(1+n)n\right] - n\pi r^2\} \tag{3}$$

where M_r is the mass of rings, r the width of the rings, D the diameter of the tower base, d the diameter of the top of the tower, H the height of the tower, h the spacing of rings, T the thickness of the rings and n is the number of the rings.

$$M_v = mlHt \tag{4}$$

where M_v is the mass of the vertical stiffeners, m the number of vertical stiffeners, l the width of vertical stiffeners and t the thickness of the stiffeners.

3.3. Buckling Analysis of the Tower

When wind farms or even wind turbines finish operating at the end of their lifetime, wind farm operators often consider repowering them to save funds and enhance sustainability assets. By repowering old wind turbines into a larger size, the amount of energy is increased due to the higher efficiency of new turbines. These repowered wind turbines should however, possess enhanced ultimate bearing capacity that means that offshore wind turbine towers should be upgraded in a meticulous strengthening way.

Figure 3 shows that gravity, moment and horizontal force are applied to the top of the tower stem. The tower shell needs to be designed so that it efficiently bears the gravity load and the moment created from the eccentricity of the wind turbine placed on the top of the tower and the horizontal force being the resultant of the force of wind, the current and the wave loading. Therefore, as the loading states on the wind turbine tower are complicated in engineering practice, the gravity, the horizontal force and the moment are individually applied to each tower model in order to explore the collapse mode under each respective loading state and calculate the ultimate bearing capacity of the offshore tower under operation in marine environments. For the buckling analysis, the subspace method is applied as the eigensolver to obtain buckling modes and eigenvalues in each buckling step. For the nonlinear buckling analysis, the imperfection of the tower wall is applied to the models and certain buckling modes should be employed to acquire the nonlinear buckling modes, whilst the Riks method is used to evaluate the post buckling behavior and the critical loading of each tower. Then, the reactions on the bottom and the displacements on the top are compared to obtain the optimum stiffening scheme option.

3.3.1. On the Effect of Gravity

The gravity effect is principally due to the wind turbine placed on the top of the tower. With reference to the bearing capacity of the tower an analysis is performed to study the most appropriate stiffening option. The mass of the stiffeners in all towers I, II, III and IV is 22.07t. The buckling response of the towers under gravity is shown in Figure 4. The nonlinear buckling analysis for gravity loading is depicted in Figure 5. The buckling analysis shows that the modes 1, 2 and 3 of towers I, II, III, IV occur in the y-axis direction (Figure 4). It can be seen that the first and second modes are symmetrical to each other and are global bending modes, whilst the third mode is a local mode. According to Figure 5, the nonlinear behavior of towers I and II, III, IV are different. The shell/tower wall (case I) is principally compressed from the top to the vicinity of the first top ring as shown in Figure 4. For towers II, III and IV, the shell is compressed as shown in Figure 6. Gravity versus displacement of towers I, II, III, IV under gravity of wind turbines can be shown in Figure 6. The displacements in the x-axis in Figure 6 depict the displacement in the y direction and the reaction force is the resultant at the tower bottom. According to Figure 6, the bearing capacity of tower I is 1.08×10^8 N, whereas the bearing capacities of towers II, III and IV are close to 1.18×10^8 N. Therefore, comparing the peak of the curves and the bearing capacities of gravity of towers II, III and IV are close each other, whilst the bearing capacity of tower I is less than those of towers II, III and IV. It can be concluded that vertical stiffeners, T-shaped stiffeners and orthogonal stiffeners are more appropriate stiffening options than rings for gravity bearing capacity.

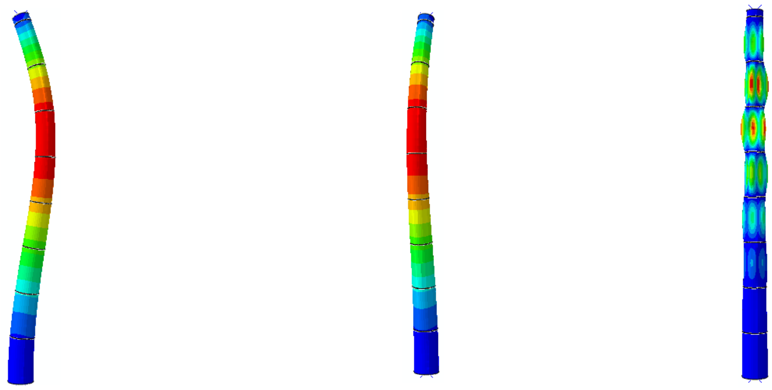

(a) (b) (c)

Figure 4. Buckling analysis of Tower I under gravity load. (a) Mode 1, (**b**) Mode 2, (**c**) Mode 3.

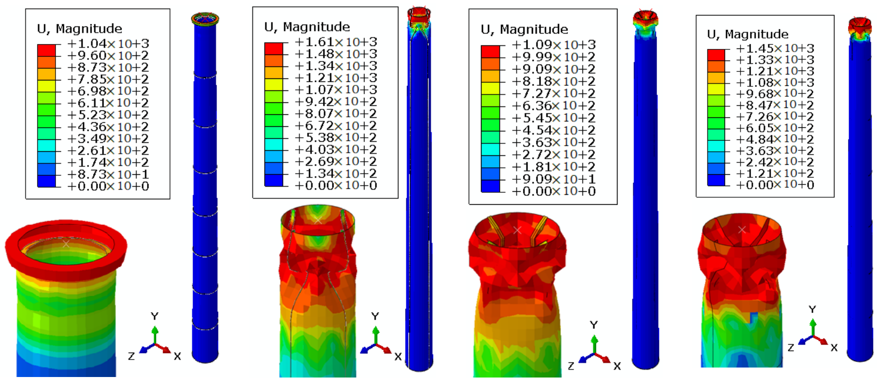

(**a**) (**b**) (**c**) (**d**)

Figure 5. Post buckling behavior of Towers I, II, III, IV under gravity loading: (**a**) Tower I, (**b**) Tower II, (**c**) Tower III, (**d**) Tower IV, (in mm).

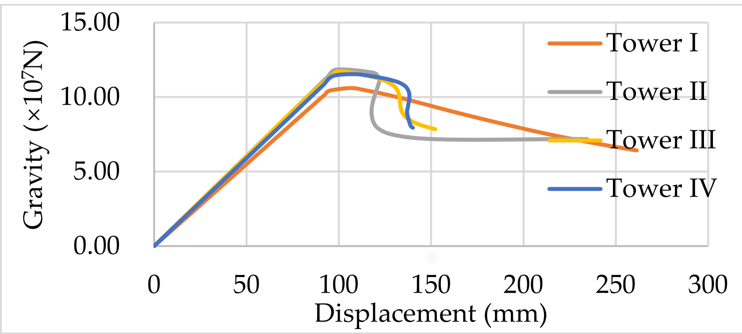

Figure 6. Gravity versus displacement of Towers I, II, III, IV under gravity load

3.3.2. On the Effect of the Horizontal Actions

Taking into consideration the horizontal forces' action on the nacelle/top of the tower, the buckling analysis of tower I is presented in Figure 7, whilst the nonlinear buckling responses of towers I, II, III, IV are depicted in Figure 8, whilst in Figure 9 the horizontal force versus displacements of towers I, II, III, IV are presented. The displacements in the *x*-axis in Figure 9 represent the horizontal displacements along the x-direction that is shown in Figure 8 (tower top) and the reaction force is the result at the tower root. It can be observed that modes 1, 2 and 3 are local modes in the vicinity of the tower base and they are similar to those of Figure 7. For post buckling behavior, the towers can translate in the *x*-axis direction due to the horizontal force. The maximum post buckling displacement of tower I is less than that of towers II, III and IV (Figure 8). According to Figure 9, the bearing capacity of towers I and IV are, respectively, 1.1×10^8 N and 1.2×10^8 N and the bearing capacity of towers II and III are close to 1.25 $\times 10^8$ N. The bearing capacity in the horizontal force of tower I is less than that of towers II, III and IV (Figure 9), whilst the bearing capacity in horizontal force of towers II and III are greater than those of towers I and IV. Therefore, towers II and III could be selected as a more appropriate option for a tower stiffened as such.

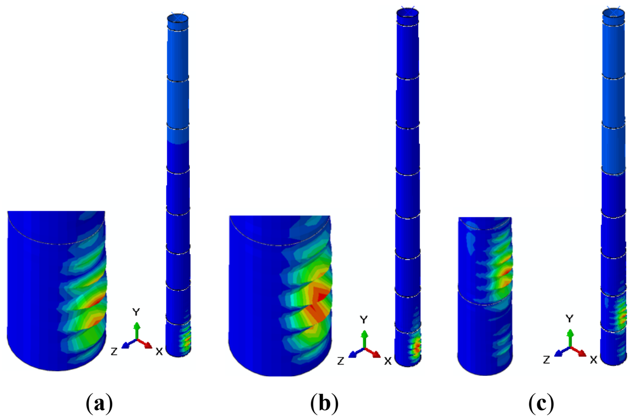

Figure 7. Buckling analysis of Tower I under horizontal force. (**a**) Mode 1, (**b**) Mode 2, (**c**) Mode 3.

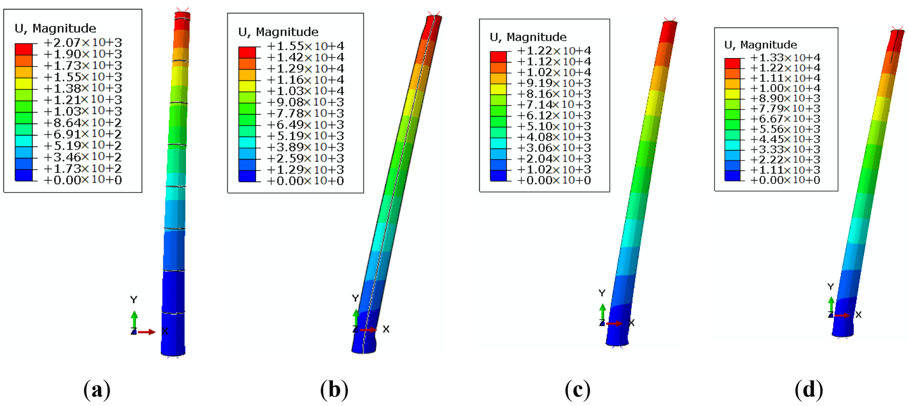

Figure 8. Post buckling behavior of towers I, II, III, IV under horizontal force. (**a**) Tower I, (**b**) Tower II, (**c**) Tower III, (**d**) Tower IV, (in mm).

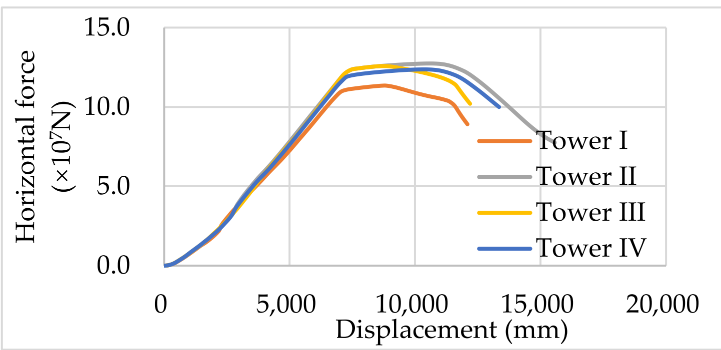

Figure 9. Horizontal force versus displacement with regard to Towers I, II, III, IV.

3.3.3. On the Effect of the Eccentricity

The eccentricity of the wind turbine that is placed on the top of tower from the center of the cross section of the tower leads to the development of an additional bending moment on the structure. With reference to this additional bending moment due to eccentricity, the buckling behavior of tower I is shown in Figure 10; modes 1, 2 and 3 of tower I are local modes in the vicinity of the tower top. Post buckling analysis of towers I, II, III, IV under moment is presented in Figure 11. Nonlinear buckling behavior of towers I, II, III, IV under moment leads to local bending modes and maximum deformation occurs on tower I. The graph of moment versus rotation of towers I, II, III, IV is presented in Figure 12. The rotation in *x*-axis in Figure 12 represents the rotation angle around the z-direction in Figure 11 of the tower top and the reaction force is the resultant of the tower bottom. According to Figure 13, the bearing capacity of towers I, II, III, IV are, respectively, 9.5×10^{10} N·mm, 1.0×10^{10} N·mm, 1.05×10^{10} N·mm and 1.05×10^{10} N·mm. Therefore, the bearing capacity of tower I is the minimum and the bearing capacity of towers III and IV are greater than those of tower II. It can be concluded that T-shaped stiffeners and orthogonal stiffeners are the optimal stiffening option for the tower under investigation.

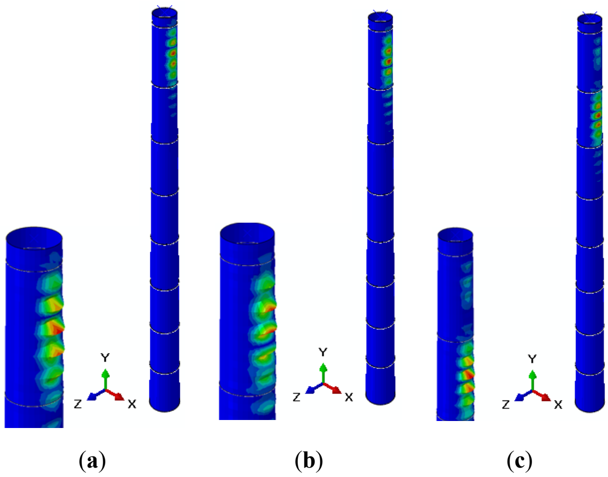

Figure 10. Buckling analysis of Tower I: (**a**) Mode 1, (**b**) Mode 2, (**c**) Mode 3.

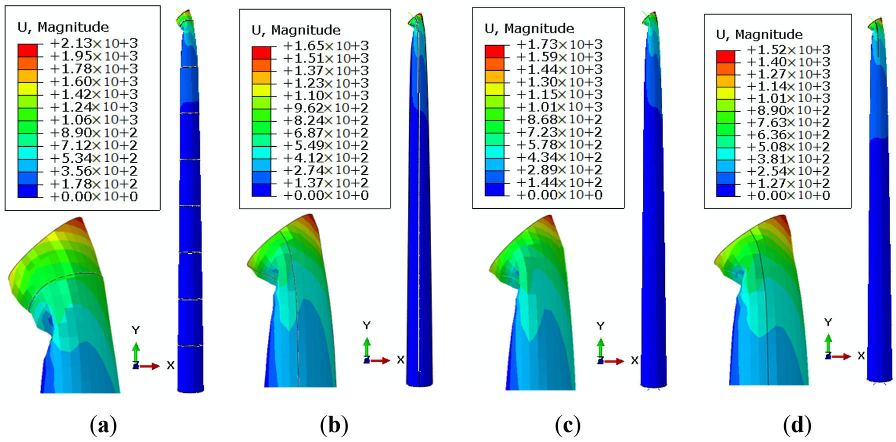

Figure 11. Post buckling behavior of Towers I, II, III, IV: (**a**) Tower I, (**b**) Tower II, (**c**) Tower III, (**d**) Tower IV, (in mm).

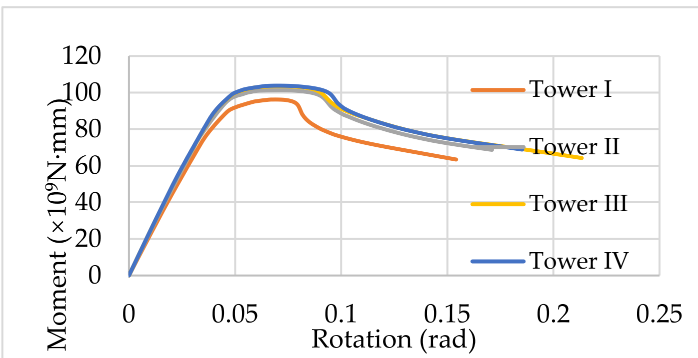

Figure 12. Moment versus rotation of Towers I, II, III, IV.

4. Conclusions

In the buckling analysis, gravity, horizontal forces and moments are, respectively, considered as the loadings that cause the collapse of the tubular towers due to buckling. Imperfections are also imported to the tubular tower models to obtain the respective nonlinear buckling modes. The bearing capacity of the towers with four different stiffening schemes are compared each other to obtain the optimum stiffening option, and it is concluded that the stiffening ring is the weakest option as a strengthening technique to avoid buckling collapse, whilst the T-shaped stiffener scheme is the most appropriate stiffening option and to enhance the strength of the tubular tower, the vertical stiffener, the T-shaped stiffener and the orthogonal stiffener schemes are better options than the ring schemes.

Funding: The first author acknowledges with thanks the research financial support provided by National Natural Science Foundation of China (No. 51808335). The financial support of the present research activity by the European Union's Horizon 2020 Research and Innovation Programme under the Marie Sklodowska-Curie Grant Agreement No 793316 is also gratefully acknowledged by the first and third authors. The third author acknowledges also with thanks the IGI Global Challenges Funding Scheme of the University of Birmingham (Project Nr 3035).

References

1. Arapogianni, A.; Moccia, J. Wind in Our Sails: The Coming of Europe's Offshore Wind Energy Industry; European Wind Energy Association: Brussels, Belgium, 2011.
2. Stavridou, N.; Efthymiou, E.; Gerasimidis, S.; Baniotopoulos, C.C. Investigation of stiffening scheme effectiveness towards buckling stability enhancement in tubular steel wind turbine towers. Steel Composite Structure, 19, 1115–1144. (2015).
3. Gkantou, M.; Rebelo, C.; Baniotopoulos, C. Life Cycle Assessment of Tall Onshore Hybrid Steel Wind Turbine Towers. Energies, 13, 3950. (2020).
4. Hu, Y.; Yang, J.; Baniotopoulos, C. Study of the Bearing Capacity of Stiffened Tall Offshore Wind Turbine Towers during the Erection Phase. Energies, 13, 5102. (2020).
5. Hu, Y., Yang, J., Baniotopoulos, C., Wang, X., Deng, X. Dynamic analysis of offshore steel wind turbine towers subjected to wind, wave and current loading during construction, Ocean Engineering, 216, 108084. (2020).
6. Hu, Y., Yang, J., Baniotopoulos, C. C. Repowering steel tubular wind turbine towers enhancing them by internal stiffening rings. Energies, 13(7), 1538. (2020).
7. Hu, Y., Yang, J., Baniotopoulos, C. C., Wang, F. A comparison of structural performance enhancement of horizontally and vertically stiffened tubular steel wind turbine towers, Structural Engineering and Mechanics. An International Journal, (73): 487-500. (2020).
8. Hu, Y., Baniotopoulos, C., Yang, J. Effect of internal stiffening rings and wall thickness on the structural response of steel wind turbine towers. Engineering Structures, 81:148–161. (2014).
9. Hu, Y., Yang, J., Baniotopoulos, C., Wang, X., Deng, X. Tall Offshore Steel Wind Turbine Towers under Wind, Current and Wave Loading: An Experimental and Numerical Study, XI International Conference on Structural Dynamics, Athens, Greece, 22-24 Nov. (2020).
10. Jay, A.; Myers, A.T.; Mirzaie, F.; Mahmoud, A.; Torabian, S.; Smith, E.; Schafer, B.W. Large scale bending tests of slender, tapered, spirally welded steel tubes. Journal of Structure Engineering, 142, 04016136. (2016).
11. ABAQUS/Standard and ABAQUS/Explicit-Version 6.8-1; Abaqus Theory Manual, Dassault System: Vélizy-Villacoublay, France, 2008. Available online: https://www.doc88.com/p-439722564721.html. Last accessed on 26/09/2020.